ELSEVIER

Chemistry and Physics of Lipids
102 (1999) 107–121

CPL
CHEMISTRY AND PHYSICS OF LIPIDS

www.elsevier.com/locate/chemphyslip

Functional analysis of acid and neutral sphingomyelinases in vitro and in vivo

Wilhelm Stoffel *

Laboratory of Molecular Neurosciences, Institute of Biochemistry, University of Cologne, Joseph-Stelzmann-Strasse 52, 50931 Köln, Germany

Abstract

The molecular cloning and the elucidation of the gene structures of the acid (aSMase) and a neutral sphingomyelinases (nSMase) of mouse and human facilitated the structural and functional analysis of these enzymes responsible for the catabolism of sphingomyelin present ubiquitously in the membrane lipid bilayer of mammalian cells. The protein and enzymic properties of the glycoprotein aSMase and of a non-glycosylated nSMase residing in the membranes of the endoplasmic reticulum have been analysed in the native as well as in the recombinant shingomyelinases. Important insight was gained from gene targeting experiments in which an aSMase deficient mouse line was generated which mimics the neurovisceral form of the human Niemann–Pick disease. The availability of the cloned aSMase and nSMases discovered so far led to a genetic approach to the verification of the concept that these enzymes in the 'sphingomelin cycle' are responsible for the generation of ceramide regarded as a lipophilic second messenger in the intracellular signal cascades activated by e.g. TNF-α, Fas ligand or cellular stress. All the available evidence derived from the aSMase deficient mouse line and several cell lines overexpressing aSMase and nSMase questions a role of ceramide released by the mammalian sphingomyelinases known so far in intracellular signal transduction.

Keywords: Acid and neutral sphingomyelinases; Sphingomyelin; Ceramide and tumor necrosis factor-α; Gene targeting

1. Introduction

Sphingomyelin (SPM) is one of the main constituents of the lipid bilayer of plasma membranes and lysosomal membranes. The long chain base sphingosine (4t-sphingenine, and dihydrosphingosine (sphinganine) are acylated with long chain fatty acids and form ceramide, the hydrophobic backbone of the large class of sphingolipids. SPM has the polar head group phosphocholine in common with the most abundant phospholipid phosphatidylcholine. SPM is strongly associated in membranes with cholesterol.

Beyond its structural functions the catabolic SPM cycle with acid (aSMase) and neutral sphingomyelinases (nSMase) as main players has gained increasing attention because ceramide, their first degradation product, is regarded as a lipid second messenger in cellular signaling upon

* Fax: +49-221-478-6882.
E-mail address: wilhelm.stoffel@uni-koeln.de (W. Stoffel)

0009-3084/99/$ - see front matter
PII: S0009-3084(99)00079-1

tumor necrosis factor-α (TNF-α), interleukin (IL) 1, vitamin D3, similar to diacylglycerol which activates different pathways leading to apoptosis, differentiation and cell proliferation. Sources of ceramide production are (a) aSMase in the lysosome and (b) liberation of ceramide from SPM by neutral SMase residing in the plasma membrane.

Acid sphingomyelinase (ASM) (sphingomyelin phosphodiesterase, E.C.3.1.4.12) is present in lysosomes of all cells where it degrades SPM of endocytosed membranes, whereas nSMase resides in the plasma membrane (Rao and Spence, 1976; Spence, 1993) and is particularly highly expressed in central nervous tissue (Barenholz et al., 1966).

The knowledge of the molecular structure and regulation of the sphingomyelinases is pivotal to our molecular understanding of their function in cellular metabolism and cell signaling. This report describes: (a) the recent advances in the characterization and functional analysis of aSMase on the protein level; and (b) the generation and properties of a null allelic aSMase mouse line generated by gene targeting. This mutant proves to be a mimicry of the type A form of Niemann–Pick disease (NPD) of human. It allows a critical analysis of the function of aSMase in the signaling pathways of normal (wt) and *asmase*$^{-/-}$ mice; and (c) the cloning and functional properties of a long sought nSMase of mouse and human.

2. Mouse and human aSMase

2.1. aSMase is a glycoprotein with specific functions of its N-glycosylation sites

Glycosylation by N-linked oligosaccharides is known to play a crucial role in glycoprotein stability and correct folding and needed to maintain enzymatic activity. Murine aSMase is a lysosomal glycoprotein with six potential N-glycosylation sites. The functional role of each individual oligosaccharide chain was analyzed (Newrzella and Stoffel, 1992). By expression of mutagenized cDNA constructs it was demonstrated that all six potential *N*-glycosylation sites are modified. Incomplete glycosylation of the most C-terminal site results in two isoforms with slightly different molecular masses. Oligosaccharides at N-84, N-173, and N-611 were found to be of minor importance for enzymatic activity, whereas a glycosylation defect at N-333 or N-393 reduces the enzymatic activity to 40% and at N-518 to less then 20%. The K_m, value of these mutants remained unaffected. Glycosylation at N-333 and N-393 mainly contribute to the enzyme stability. These mutants loose rapidly their enzymatic activity and are degraded during incubation of cell extracts at acidic pH. In contrast, aSMase deficient in N-518 linked oligosaccharide shows only a moderately reduced activity while the protein is rapidly degraded. Apparently, translation of this mutant results in a substantial amount of enzymatic inactive and proteolytic sensitive protein, indicating an improper protein folding. This mutant is also significantly degraded, when trapped in the ER/cis-Golgi by Brefeldin A administration. To enable the correct targeting to the lysosomal compartment, aSMase is phosphorylated at mannose residues of certain oligosaccharides. Quantification of $^{32}PO_4$ pulse labelled glycosylation mutants revealed a predominant involvement of the oligosaccharides linked to N-84, N-333, and N-393. Insufficiently glycosylated aSMase forms a stable complex with Ig heavy chain binding protein (Bip) and thus remains in the ER.

2.2. Gene structure of mouse and human aSMase

The recent isolation and characterization of the *human aSMase*, the cloning and sequencing of the cDNA (Quintern et al., 1989), and the coding sequence of the human gene (Schuchman et al., 1991; Newrzella and Stoffel, 1992) revealed that aSmase is a 627 amino acid residue glycoprotein of 64 kDa which is encoded in six exons. The gene is distributed over approximately 5 kb in the *asmase* locus on chromosome 11p15.1–15.4 (Pereira et al., 1991).

The complete *mouse aSM gene*, Fig. 1a, was isolated and subcloned in pUC19 as a 4.8-kb BamHI fragment, starting 780 bp upstream the start codon and ending 160 bp downstream the polyadenylation signal (Newrzella and Stoffel, 1992, # 4). The human aSMase gene was isolated and subcloned in pUC19 as a 3.2 kb BamHI

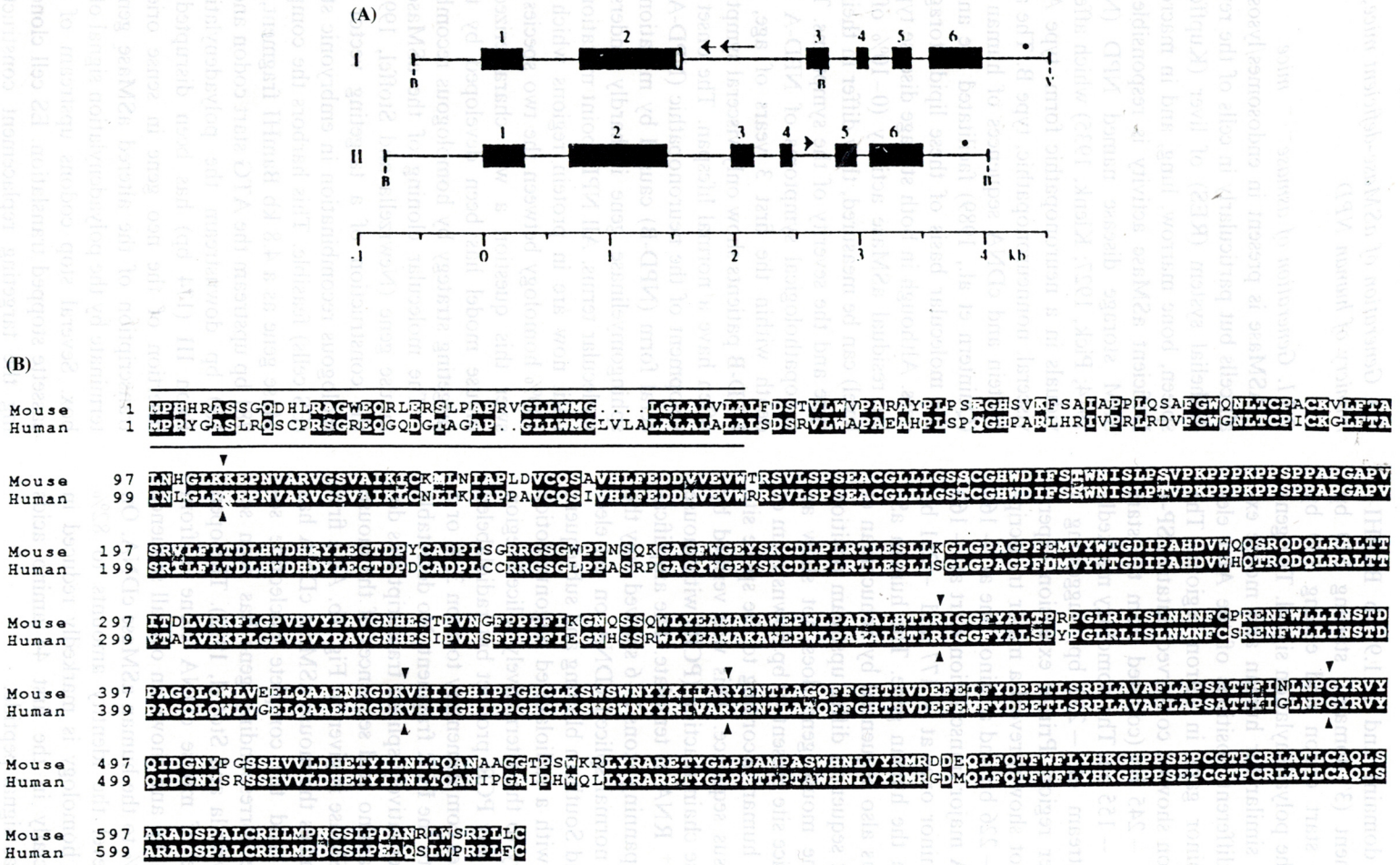

Fig. 1. (A) Gene structure of human acid sphingomyelinase (ASM) (I) and mouse ASM (II). Arrow: Alu1 element; □, alternative splice region in the human gene; ○, polyadenylation signal; B, BamHI restriction site; V, EcoRV restriction site. (B) Comparison of the ASM amino acid sequence of mouse and human. Lines mark the signal peptide according to the van Heijne algorithm; arrow heads mark the exon boundaries.

fragment (5′ domain) and a 1.9 kb BamHI–EcoRV fragment (3′ domain), starting 520 bp upstream the start codon and ending 180 bp downstream the polyadenylation signal. The gene structures are similar for human and mouse except for the different positions of the AluI elements and minor gaps in intron regions. The promoter region shows a conserved putative SP-1 site at about −245 bp (counted from the start codon) and at −155 bp. The homology markedly decreases upstream of −250 bp, suggesting a short promoter region. Primer extension experiments (data not shown) reveal a major transcription start at −226 bp and a minor one at −160 bp for mice. A major transcription start at −160 bp and two minor ones at −177 and −251 bp were found in the human gene. The human aSMase gene was also sequenced by Schuchman et al. (1991), but sequences differ upstream position −210 bp. The mouse gene does not show an alternative splice site present 40 bp downstream of exon 2 of the human according to the splice site donor consensus sequence. This was verified by RT-polymerase chain reaction (PCR) with mouse brain poly(A)$^+$ RNA as template. The amplification product spanning exons 2–6 showed only the length of the normal spliced cDNA on gel electrophoresis and Southern blotting and subsequent hybridisation with a radiolabeled oligonucleotide complementary to the alternatively spliced region did not mark any PCR product but radiolabeled oligonucleotides complementary to exon 3, 4, or 5 bind strongly to the PCR fragment. No detectable amount of alternatively spliced transcript was detectable. The amino acid sequences of the mouse and human aSMase is given in Fig. 1b. As a first step in the studies the mouse aSMase cDNA has been isolated and the complete nucleotide sequence of the corresponding gene has been sequenced (Newrzella and Stoffel, 1992). The open reading frame of mouse cDNA clone is from −118 to 2221 bp and shows an overall sequence identity of 81% to the human aSMase cDNA. On the peptide level the identity amounts to 82% (Fig. 3). The homology is markedly reduced in exon 1, especially in the first 44 amino acids determinated as signal peptide.

2.3. Generation of aSMase-deficient mice, a mimicry of human NPD

2.3.1. Generation of asmase$^{-/-}$ mice

ASMase is present in endosomes/lysosomes of all cells but particularly in cells of the reticuloendothelial system (RES) of liver (Kupffer cells), spleen, bone marrow, lung, and in macrophages. Deficient aSMase activity is responsible for the SPM storage disease named NPD (Niemann, 1914; Pick, 1927; Klenk, 1935) which affects individuals in a neuronopathic form, type A, and a visceral, nonneuronopathic, type B. The available protein and cDNA sequences of human aSMase (Quintern et al., 1989) facilitated the analysis of the molecular basis of these lipid storage disorders. Although in both storage disease types similar residual aSMase activity (0–10% of normal level) can be measured, they differ in their phenotype and the severity of the symptoms. The neuronopathological symptoms of NPD-A leads to death within the first 3 years of age, whereas NPD-B patients show only visceral symptoms and often have a normal lifespan. The onset and development of the neuronopathic (NPD-A) or visceral form (NPD-B) caused by mutations of the sphingomyelinase gene is hardly understood in molecular terms. All NPD point mutations found until now are in protein regions which show a 100% homology between the two species. To answer this question a well characterized NPD-mouse model has been developed by the gene targeting strategy by homologous recombination.

The molecular cloning of the aSMase of the mouse gene (Newrzella and Stoffel, 1992) made the construction of a targeting vector for homologous recombination in embryonic stem cells (ES cells) feasible. This harbors the complete aSMase gene as a 4.8 kb BamHI fragment, starting 781 bp upstream the ATG start codon and ending 160 bp downstream the polyadenylation site. Exon III (174 bp) has been disrupted by the insertion of the neo gene in sense orientation, transcription of the altered aSMase gene which terminate by the polyadenylation signal of the neo box. Several stop codons upstream of the neo cassette stopped translation. ES cell clones carrying the targeting replacement construct in the

asmase locus were obtained by electroporation and transferred into blastocysts of C57BL/6 donors which were used for the generation of male chimeric mice. Cross breeding of chimeric males with C57BL/6 females yielded heterozygotes which were intercrossed to obtain homozygous mutant mice. For allelic typing of transgenic mice genomic DNA of ES cells and tail DNA of chimeric mice of heterozygous and homozygous offsprings was digested with EcoRI and analyzed by Southern blot analysis using the 3′- and neo-probe. The release of a 3 kb EcoRI fragment indicated the mutant allele, a 2.3 kb fragment the wild type allele, respectively.

The homologous recombination event was further confirmed by PCR analysis with the 5′ and 3′ primers.

2.4. Characterization of aSMase deficiency in asmase$^{-/-}$ mutant mice: aSMase mRNA is absent in all organs

2.4.1. Development of asmase$^{-/-}$ mice

The *aSMase* mutant mice developed indistinguishably from the wild type for a period of 8–10 weeks, when the homozygous mutant mice developed a whole body tremor and a severe intention tremor, their gait became increasingly ataxic, tottering with zig-zag movement, characteristic for cerebellar dysfunction.

Hepatosplenomegaly becomes visible around day 60 after birth. In the final stage around day 120 after birth the mutant mice show a severe pulmonary distress which leads to largely restricted physical activity and finally to death. The life expectancy of aSMase-deficient mice is around 4–6 months.

2.5. Complete lack of aSMase but not nSMase activity in homozygous aSMase mutant mice

aSMase was assayed in the total protein extract of liver, spleen, and brain of wild type mice, hetero- and homozygous mutants by release of the water soluble (N-$^{14}CH_3$-choline) phosphorylcholine group from (N-$^{14}CH_3$-choline) SPM. A reduction of aSMase activity to one half was measurable in the heterozygous mutants but no activity in the homozygous mutant, Table 1A.

Table 1
Enzyme activity of acid sphingomyelinase (aSMase) in wild type, hetero (+/−) and homozygous (−/−) mice (A) and comparison of the enzyme activity of aSMase and neutral sphingomyelinase (nSMase)[a]

(A)	Genotype	Protein (μg)	dpm	% Activity	Spec. activity
Liver	+/+	3; 5	3410; 6035	100; 100	100
	+/−		2395; 1535	70; 42	
	−/−		0; 0	0; 0	
Spleen	+/+	3; 5	1535; 5235	100; 100	80
	+/−		1395; 2120	55; 40	
	−/−		0; 0	0; 0	
Brain	+/+	3;5	6525; 14 215	100; 100	210
	+/−		3850; 9720	59; 68	
	−/−		0; 0	0; 0	
(B)	Genotype	Protein (μg)	aSMase (dpm)	nSMase (dpm)	
Liver	+/+	25	8743; 8464	2728; 1931	
	−/−		0; 0	317; 371	
Spleen	+/+	25	3322; 3860	897; 741	
	−/−		0; 0	261; 309	
Brain	+/+	25	10 076; 10 922	27 762; 29 646	
	−/−		0; 0	20 101; 26 602	

[a] Enzyme activity is expressed in dpm. N-$^{14}CH_3$-phosphocholine released from N-$^{14}CH_3$-choline sphingomyelin (SPM).

Residual nSMase was assayed in extracts of plasma membrane enriched fractions (600 × *g* supernatant) of liver, spleen, lung, and brain under neutral reaction conditions, pH 7.4. The analyses of aSMase with the homogenates as enzyme source match those obtained with the 100 000 × *g* supernatant of liver, spleen, and brain of wild type, *asmase*$^{+/-}$ and *asmase*$^{-/-}$ mice. A total of 25–30% of aSMase activity of the respective tissue is still measurable at pH 7.4 under the assay conditions for nSMase. This has been demonstrated with purified human aSMase (unpublished). Therefore the numbers in Table 1B for nSMase activity of *asmase*$^{+/-}$ and *asmase*$^{-/-}$ mice must be corrected by this contribution of aSMase. The SMase activity in *asmase*$^{-/-}$ liver, spleen, and brain therefore reflects the actual nSMase activity in the respective tissue. Thus nSMase activity is apparently not altered by the loss of aSMase expression.

Interestingly, Table 1B indicates that nSMase activity in the brain of wild type mice is three times higher than aSMase activity. nSMase in homozygous *asmase*$^{-/-}$ mice is only slightly reduced as compared to parenchymous tissues rich in RES such as spleen, liver, and lung.

2.5.1. Lipid analysis of wild type mice and hetero- and homozygous mutant mice

Sphingomyelinase-deficient mice store large amounts of SPM in RES cells. Total lipids of liver, spleen, and brain, which are of central interest in NPD-A and -B were extracted from liver, spleen, and brain specimen of wild type, hetero- and homozygous mutant mice with chloroform–methanol and analyzed by thin layer chromatography (TLC). Esterlipids of the total lipid extracts were also saponified to water soluble potassium salts of fatty acids and the polar head group components (glycerolphosphate, and the respective bases).

The most prominent lipid in liver and spleen of homozygous mutant mice is SPM. The accumulation of SPM is also visible in the lipid extract of brains although by far not as pronounced as in the RES of liver and spleen.

2.6. Histology of homozygous aSMase (−/−) mice visualizes massive lipid deposits throughout RES-system

Inspection of the parenchymous organs of homozygous aSMase-deficient mice revealed very frequently enlarged liver and spleen with an increase of wet weight of total liver to 1.5 times, that of spleen varied but often reached twice the weight of age- and sex-matched wild type mice in the final stage.

In histology Kupffer cells of liver and hepatocytes formed foam cells with extended cytoplasmic vacuolation (Otterbach and Stoffel, 1995). In electron microscopy the Kupffer cell of a liver acinius of a *wild type* and homozygous *asmase*$^{-/-}$ mutant mouse, given here as a representative example, shows the foam cell morphology (Fig. 2). Lysosomes are filled with stacked membranes of stored SPM forming myelin figures.

Alveoli of the lung of homozygous mice are clotted with infiltrations which consist of lipid loaded histiocytes.

Ganglion cells of homozygous mice in grey matter of the central nervous system (CNS) contain frequently swollen pale vacuolation in cytoplasm (Otterbach and Stoffel, 1995; Kümmel et al., 1997), Fig. 2.

The endothelium of plexus chorioideus is swollen and heavily loaded with foam cells and likewise the spinal fluid space between the plexus.

The most striking observation was the progressive degeneration of the Purkinje cells, which occurs within 60–90 days after birth in homozygous mice, Fig. 3.

2.7. Locomotor ataxy in aSMase mutant mice

Cerebellar locomotor ataxy with a straddle-leg gait and the intention tremor are the dominant neuropathological symptoms.

All the experimental evidence pointed out that we had generated an aSMase deficient mouse line by gene targeting. This novel strain of mutant mouse mimics the lethal, neurovisceral form of the human SPM storage disease, known as NPD. Homozygous mice accumulate extensively SPM in the RES of liver, spleen, bone marrow, lung, and

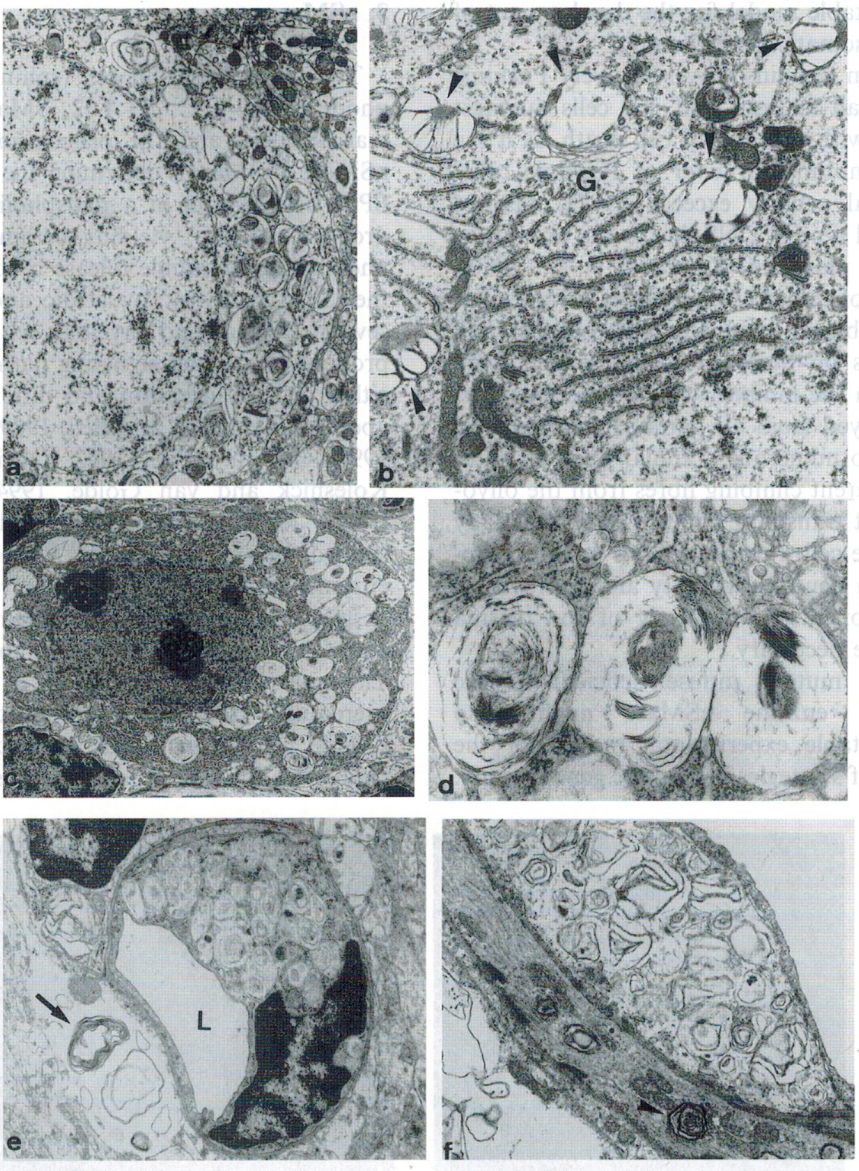

Fig. 2. Neuronal storage in cerebral and cerebellar cortex of the neurovisceral type A (NPA) mouse (electron microscopy). Cerebral cortex from a 100-day-old NPA mouse. (a) Large neuron and (b) Purkinje cells of an 18-day-old mouse with membrane-bound cytoplasmic inclusions. (c) Purkinje cell of a 100-day-old NPA mouse. (d) Magnification of lysosome from c. (e) Small cerebral capillary with excentric cushion-like thickening of the endothelium stuffed with lysosomal storage material. Obliteration of vascular lumen (L) and storage material in an astrocytic process (arrow). (f) Arteriole with endothelial storage material and smooth muscle cell containing single lysosomal inclusions (arrowhead). a, b, c: × 9200; e: × 28 000; f: × 13 000.

in brain. Most strikingly, the ganglionic cell layer of Purkinje cells of cerebellum degenerates completely, leading to severe impairment of neuromotor coordination. The 'Niemann–Pick mouse' facilitates studies on the function of aSMase in the generation of ceramide as proposed second messenger in the intracellular signalling pathways and across the plasma membrane. Furthermore, it

provides a suitable model for the development of strategies for somatic gene therapy.

The question remains why selectively Purkinje cells and not all neurons and glia cells manifest SPM storage with subsequent cell death. Is it the enhanced membrane turnover of Purkinje cells? Their neuronal activity exceeds by far that of most other cell type of CNS due to the prominent role in motor plasticity (Konnerth et al., 1990). Purkinje cells of the cerebellar cortex form excitatory and inhibitory synapses with parallel and climbing fibres on the excitatory side and from basket cells on the inhibitory side. Sensory information is relayed from all parts of the body via mossy fibres to numerous granular cells. In addition single afferent climbing fibres from the olivocerebellar tract transmit excitatory inputs directly to the Purkinje cell. Further studies on the correlation between neuronal activity and turnover of cellular components, particularly of the plasma membrane, are necessary.

Finally the mutant mouse deficient in the 'housekeeping' enzyme aSMase might also provide a suitable experimental model for the development of strategies in somatic gene therapy.

3. nSMase

Two sphingomyelinases (sphingomyelin phosphodiesterase E.C. 3.1.4.12, SMase), the lysosomal aSMase, and the plasma membrane-bound nSMase (nSMase), determine the major route of SPM degradation in a phospholipase C-like hydrolysis reaction, yielding ceramides and phosphocholine. Ceramide release by the activation of the 'SPM pathway' by acidic and/or nSMase in several normal and myeloid cell lines has been proposed to trigger signaling pathways leading to either cell proliferation and differentiation or to apoptosis (Hannun and Bell, 1989; Dressler et al., 1992; Olivera et al., 1992; Obeid et al., 1993; Kolesnick and van Golde, 1994; Divecha and Irvine, 1995; Hannun and Obeid, 1995). As described before aSMase is a well characterized enzyme. nSMase, however, has remained elusive despite several purification attempts (Chatterjee and Ghosh, 1989; Maruyama and Aima, 1989). The molecular characterization of this enzyme is a prerequisite for understanding the role of ceramide in cellular signal transduction processes mediating the response to agonists like TNF-α,

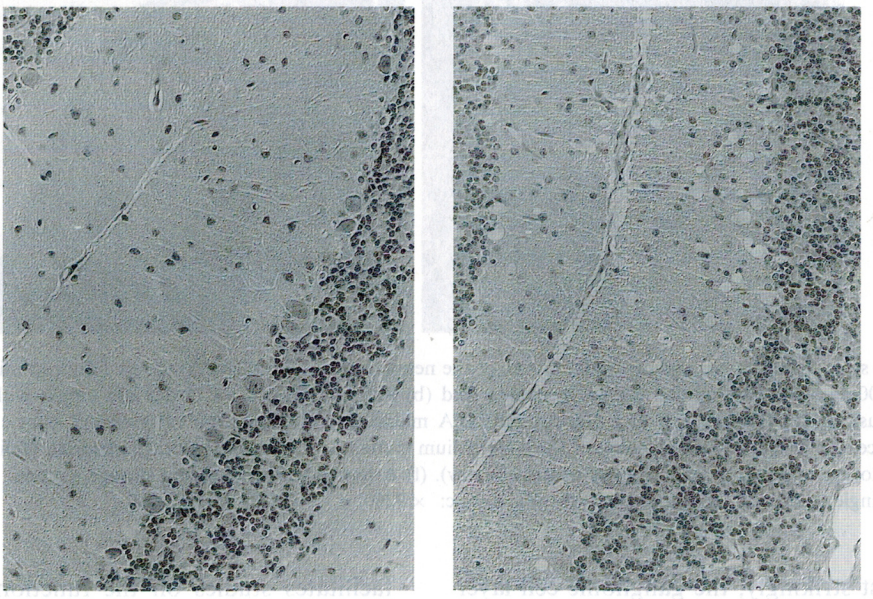

Fig. 3. Cerebellar cortex of the neurovisceral type A (NPA) mouse (light microscopy). Left: a 100-day-old wild type animal with normal configuration of the cerebellar cortex. Right: a 100-day-old NPA mouse showing extensive reduction of Purkinje cells and numerous macrophages in the molecular layer. Luxol fast blue-cresyl violet, interference contrast, a, b: × 250.

IL-1β, interferon-γ (IFN-γ) and 1α,25 dihydroxyvitamin D_3. Previous studies addressing this question administered membrane-permeable ceramides substituted with short chain fatty acids which have potentially membrane-toxic side effects, other studies used bacterial sphingomyelinases. Bacterial sphingomyelinases are soluble enzymes and are likely to generate ceramide in other subcellular compartments than the one accessed by the plasma membrane-bound mammalian nSMase. They also lack the regulatory features of their mammalian counterparts.

We succeeded recently in the cloning, identification and functional characterization of a mouse and human nSMase. This enabled us to study the function of nSMase in the activation of the SPM cycle in response to the challenge of stably expressing cell lines (HEK293 and the myeloid leukemia cell line U937) with TNF-α for the study of the activation of JNK2, ERK1 and nuclear transcription factor kB (NF-κB) as well as apoptosis.

3.1. Cloning of the murine and human nSMase cDNA

The approach of the unsuccessful biochemical purification of mammalian nSMase (Chatterjee and Ghosh, 1989; Maruyama and Aima, 1989) was unsuccessful. A different approach was used for the identification of this enigmatic enzyme (Tomiuk et al., 1997). *Bacillus cereus*, *Clostridi.* Their pH optima and ion requirements are similar to the plasma membrane-associated Mg^{2+}-dependent mammalian nSMase (Spence, 1993). Generalized profiles (Bucher et al., 1996) were derived from multiple sequence alignments of complete sequences or the most highly conserved regions of these bacterial SMases. In both cases profile searches in the protein sequence databases identified a single significant match in the open reading frame (ORF) YerO19w from the yeast *Saccharomyces cerevisiae*. The database of expressed sequence tags (dbEST) contained several mammalian sequences with high homology to the yeast sequence. This homology was confirmed by cloning and sequencing. The full length cDNAs were assembled from overlapping mouse and human EST sequences, respectively. Subsequent inclusion of the yeast, human and murine sequence into iterative cycles of profile construction and database searches resulted in significant matches with a large family of Mg^{2+}-dependent phosphodiesterases including exonuclease III and desoxyribonuclease I from the bacterium *Escherichia coli*. The crystallographic structure of these two nucleases allows the delineation of residues important for Mg^{2+} binding and for catalysis, as indicated in Fig. 4. They are totally conserved in the bacterial SMases, the yeast ORF and the mammalian nSMase candidates. This observation further supported credibility to this newly established superfamily. A membrane topology of nSMase schematically drawn in Fig. 5 is proposed.

The sequences of murine and human nSMase candidates are highly related. Their ORFs encode proteins of 419 residues (mouse, 47.5 kDa) and 423 residues (human, 47.6 kDa), respectively. In contrast to the bacterial SMases the mammalian cDNA-derived amino acid sequences contain no signal sequence at their N-terminus. Two adjacent hydrophobic domains at the C-terminus separated by eight amino acid residues spanning the endoplasmic reticulum (ER) membrane are suggested by the hydropathy plot. The nSMase candidates thus appear to be with their catalytic domain facing the cytosol and only a minor portion of the protein facing the luminal compartment. Bacterial SMases are secreted as soluble protein with the reported properties of mammalian Mg^{2+}-dependent nSMase. The 1.7 kb mRNA of the murine nSMase candidate appeared to be ubiquitously expressed. RNA of intestine, kidney, brain, liver, heart and lung, showed a strong signal in Northern blot hybridization analysis (Dressler et al., 1992), while the expression in spleen appeared to be low, Fig. 6. The intensities of the nSMase mRNAs did not match the observed enzymatic activity in the corresponding tissues, Table 2, which indicates a posttranscriptional regulation of nSMase by a so far unknown mechanism. No change in expression level of nSMase was observed in RNA and enzymatic activity from aSMase-deficient mice (Tomiuk et al., 1997).

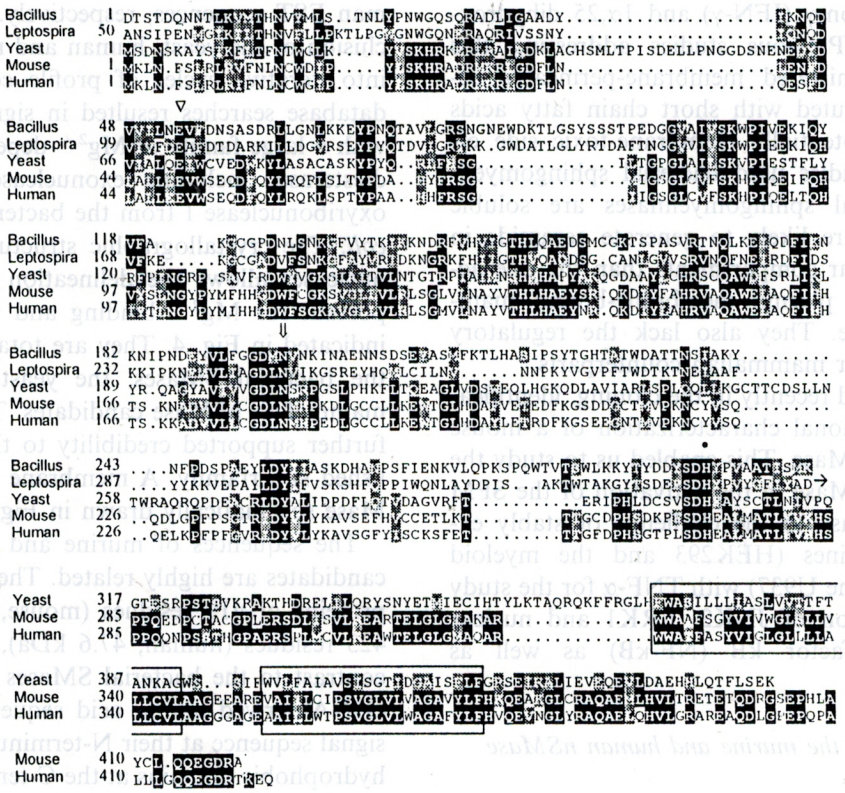

Fig. 4. Alignment of two bacterial sphingomyelinases with open reading frame (ORF) YerO19w from *Saccharomyces cerevisiae* and neutral sphingomyelinases (nSMase) from mouse and man. The first block contains the catalytic domain present in both pro- and eukaryotic nSMases, the second block contains the C-terminal extension of the eukaryotic enzymes with the two transmembrane regions boxed. Residues identical or similar in more than 50% of the sequences are shown on black or grey background, respectively. The numbering refers to the mature sequences for the secreted bacterial enzymes and to complete ORFs for the eukaryotic enzymes devoid of signal sequences. The Mg^{2+}-complexing glutamic acid (triangle), asparagine involved in substrate binding (arrow) and the general base histidine (filled circle), are indicated above the sequence.

3.2. The cloned phosphodiesterase is the long sought Mg^{2+}-dependent nSMase

HEK293 cells were transfected with the cDNA of the murine nSMase candidate and stably generated cell lines expressing the nSMase candidate protein for the comprehensive characterization of the functions. Enzymatic assays of membrane extracts showed a strong increase of the nSMase activity (specific nSMase activities between 0.3 and 10 μmol/mg protein per h). The expression level of the construct and the specific nSMase activity measured were closely correlated as visualized by RT-PCR. Western blot analysis, using the peptide-derived anti-mouse nSMase antibody, revealed a similar correlation with the amount of immunoreactive material.

Cell fractionation experiments revealed that the sphingomyelinase activity resides in the extracts of ER membrane enriched fraction of different organs. The activity does not correspond to the mRNA in these organs, Table 2. The pH-optimum was found between 6.5 and 7.5, the K_m value for long chain natural SPM amounts to $1.0–1.5 \times 10^{-5}$ M and Mg^{2+} ions are required. EDTA addition leads to a reversible complete inhibition which is reversed by Mn^{2+} and Mg^{2+} ions. Triton X-100 concentration required for optimal enzymatic activity was between 0.03 and 0.05%. nSMase activity remains unaffected by

DTT or 2-mercaptoethanol, but 20 mM glutathione completely inhibited the enzyme. Arachidonic acid (0.5 mM) activates nSMase in membrane extracts of overexpressing HEK cells. The cloned nSMase hydrolyzes the structurally related phosphatidylcholine only with a less than 3% efficiency.

The enzymatic degradation of SPM by the cloned enzyme follows a specific phosphodiesterase reaction. It does not catalyze a phosphocholine or choline transfer from SPM to diacylglycerol or phosphatidic acid or vice versa from phosphatidylcholine to ceramide. The mammalian nSMases contain a C-terminal extension relative to their bacterial homologues, including the two membrane-spanning regions. This extension is required for enzymatic activity. Truncated murine nSMase (residues 1–282) in which the two putative transmembrane domains were deleted, has lost SMase activity when expressed in HEK293 cells.

The properties and the location of cloned nSMase in the ER membrane correspond well to those reported for the nSMase in tissues, notably in brain. Therefore, the cloned phosphodiesterase which was discovered is the long sought Mg^{2+}-dependent nSMase.

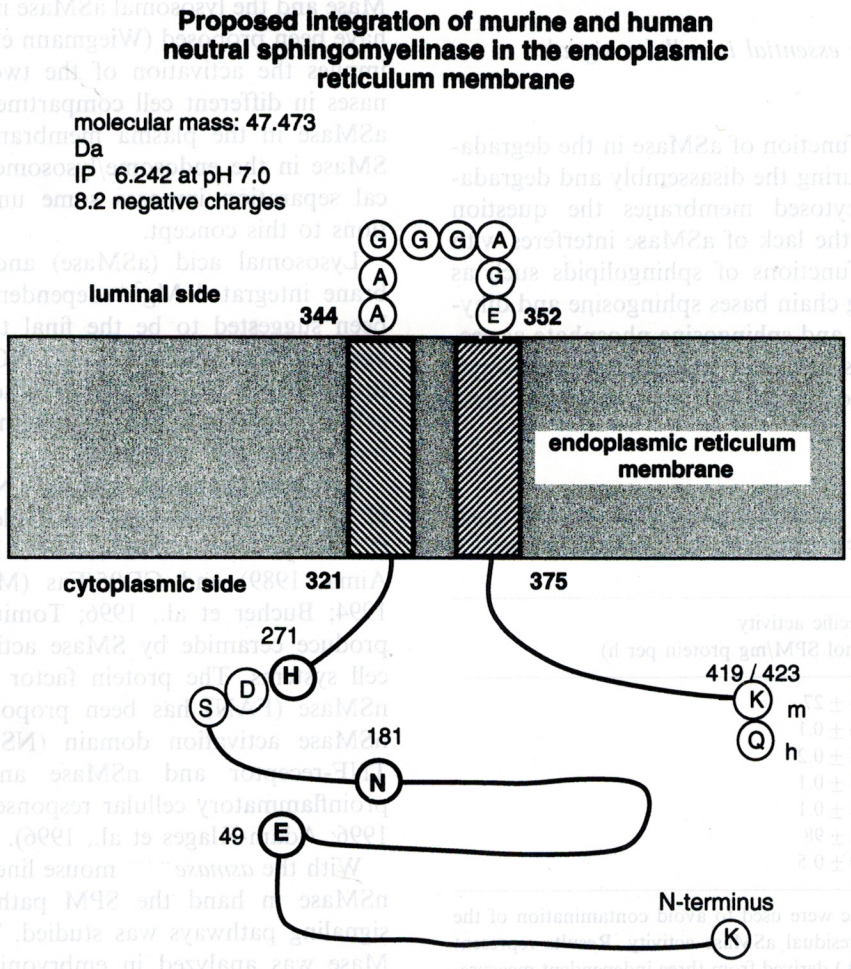

Fig. 5. Proposed ER membrane topology of neutral sphingomyelinase (nSMase).

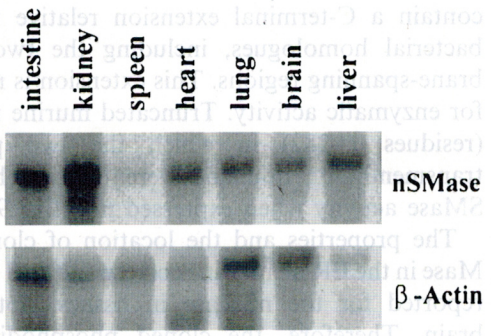

Fig. 6. Expression of neutral sphingomyelinase (nSMase) in mouse tissues. Northern blot analysis of poly-(A^+) mRNA derived from different murine tissues. The 770 bp sequence at the 5′ end of murine cDNA was used as a hybridization probe. The membrane was rehybridized with a β-actin probe for standardization.

3.3. Is nSMase essential in cellular signal transduction?

Beyond the function of aSMase in the degradation of SPM during the disassembly and degradation of endocytosed membranes the question arises whether the lack of aSMase interferes with the emerging functions of sphingolipids such as ceramides, long chain bases sphingosine and dihydrosphingosine and sphingosine phosphate as second messengers in signal transduction pathways. SPM degradation could be a main source of these intermediates.

Table 2
Specific activity of neutral sphingomyelinase (nSMase) in different tissues of acid sphingomyelinase deficient (*asmase*$^{-/-}$) mice[a]

Tissue	Specific activity (nmol SPM/mg protein per h)
Intestine	113 ± 27
Kidney	1.6 ± 0.1
Spleen	1.5 ± 0.2
Heart	4.8 ± 0.1
Lung	1.2 ± 0.1
Brain	582 ± 98
Liver	2.0 ± 0.5

[a] *asmase*$^{-/-}$ mice were used to avoid contamination of the enzyme assay by residual aSMase activity. Results represent mean value (± S.D.) derived from three independent measurements.

Ceramide-mediated cellular responses to this putative second messenger molecule are rapidly emerging (Divecha and Irvine, 1995). It has been proposed that the two sphingomyelinases with neutral and acidic pH optima respectively are activated independently by a TNF 55 kDa TNF receptor (TNF-RT) complex. aSMase supposedly triggers the nuclear translocation and activation of the NF-κB (Machleidt et al., 1994). TNF-α-stimulated release of ceramide has been implicated in the activation of membrane-activated protein kinases (Mathias et al., 1991), in the mitogen-activated protein kinase cascade (Raines et al., 1993), and in the TNF-induced cell killing (Obeid et al., 1993; Jarvis et al., 1994). Recently a functional dichotomy of the plasma membrane-bound nSMase and the lysosomal aSMase in TNF signaling have been proposed (Wiegmann et al., 1994). This implies the activation of the two sphingomyelinases in different cell compartments, the neutral aSMase in the plasma membrane and the acid SMase in the endosome/lysosome. The topological separation imposes some unanswered questions to this concept.

Lysosomal acid (aSMase) and plasma membrane integrated Mg^{2+}-dependent nSMase have been suggested to be the final target of several agonists (e.g. TNF-α, IL-1β, NGF, 1α,25 dihydroxyvitamin D_3, and INF-γ) leading to complex cellular responses such as growth arrest, cell differentiation and apoptosis.

Cytokine challenge, e.g. by TNF-α (Olivera et al., 1992; Kolesnick and van Golde, 1994), IL-1β (Chatterjee and Ghosh, 1989; Maruyama and Aima, 1989) and CD95/Fas (Machleidt et al., 1994; Bucher et al., 1996; Tomiuk et al., 1997) produce ceramide by SMase activation in some cell systems. The protein factor associated with nSMase (FAN) has been proposed to link the nSMase activation domain (NSD) of the p55 TNF-receptor and nSMase and to promote proinflammatory cellular responses (Adam et al., 1996; Adam-Klages et al., 1996).

With the *asmase*$^{-/-}$ mouse line and the cloned nSMase in hand the SPM pathway related to signaling pathways was studied. The role of aSMase was analyzed in embryonic fibroblasts of *asmase*$^{-/-}$ mice and of the cloned nSMase in

stably overexpressed in HEK293 and U937 cells. These cells were challenged with TNF-α, one of the most potent inducers of NF-κB.

Evidence was presented that aSMase is not involved in the TNF-α induced signal transduction (Zumbansen and Stoffel, 1997). TNF-α treatment induced the dissociation and degradation of IκB and the nuclear translocation of NF-κB indiscriminently in embryonic fibroblasts from wild type and *asmase*$^{-/-}$ mice.

Regarding the role of nSMase as an essential parameter of the postulated nSMase mediated signaling pathways, the following were analyzed:

(a) The kinetics of ceramide production in HEK293 and U937 cells metabolically labeled with 1-[^{14}C]palmitate. Cellular ceramide concentrations were not determined by the commonly used diacylglycerolkinase (DAGK) assay (Schütze et al., 1992) because its reliability appears questionable in the light of a recent study (Watts et al., 1997). Instead, the radiolabelling technique as described previously was used (Zumbansen and Stoffel, 1997).

Independent of the degree of nSMase expression in HEK293 cells ceramide formation upon TNF-α stimulation was identical to the level observed in mock-transfected cells.

No increase in NF-κB activation and no apoptotic features (PARP cleavage, nuclear chromatin fragmentation) were observed. In contrast, in U937 cells moderately overexpressing the nSMase construct the TNF-α-triggered ceramide formation was increased by 25% within the first 10 min and remained 15–20% above the level at zerotime or in mock-transfected cells.

(b) Similar to the study on the effect of TNF-α on aSMase-deficient mouse fibroblasts (Zumbansen and Stoffel, 1997), the kinetics of TNF-α-induced NF-κB activation in nSMase-transfected U937 cells were followed. Electrophoretic mobility shift analysis revealed kinetics identical with that of mock-transfected cells questioning a role of nSMase in NF-κB activation in this cell type.

(c) Ceramide generated by the nSMase has been proposed to trigger an anti-apoptotic pathway via a ceramide-activated protein kinase (CAPK) with the activation of the extracellular signal-related kinases (ERK) in response to TNF-α (Wiegmann et al., 1994). A significant ERK1 activation could neither be measured in mock-transfected nor in nSMase overexpressing U937 cells, nor after stimulation with TNF-α. Additionally, no difference in the activation of JNK was observed in mock-transfected and nSMase-transfected U937 cells, Fig. 7.

(d) PARP cleavage (Zumbansen and Stoffel, 1997) was taken as an indicator of apoptosis in U937 cells transfected with nSMase. However the kinetics of the occurring PARP cleavage after TNF-α/cycloheximide (CHX) stimulation was indiscriminantly in nSMase overexpressing U937 cells and mocktransfected U937 cells, Fig. 8. Treatment of the cells with TNF-α alone led only to partial PARP cleavage which remained incomplete for at least 18 h. CHX alone had no effect (data not shown). Furthermore, overexpression of nSMase had no obvious effect on cell growth and morphology.

Ceramide released by the induction of a plasma membrane-bound Mg^{2+}-dependent nSMase has also been postulated as intracellular signal for apoptosis, it has been linked to extracellular signal-regulated ERK1 cascade and proinflammatory response (Pena et al., 1997). In contrast to these reports, the nSMase-overexpressing U937 cells release only moderately elevated concentrations of ceramide upon TNF-α stimulation. No activation of ERK1 was observed.

In summary it was not possible to detect any biological effects influenced by the overexpressing of nSMase in contrast to the effects expected from studies applying membrane-permeable ceramides and bacterial nSMase. Whether the mammalian nSMase gives rise to more pronounced effects in very specific cell types and/or requires particular activating factors in vivo that were not present in sufficient amounts in the experiments described here awaits clarification. This hypothesis is supported by the observation that even HEK-cells highly overexpressing nSMase show no obviously altered rate of SPM hydrolysis compared to mock-transfected cells probably due to an effective inhibition (regulation) of the enzyme activity in the plasma membrane.

nSMase shows by far the highest enzymatic activity of all tissues in the CNS. This suggests a

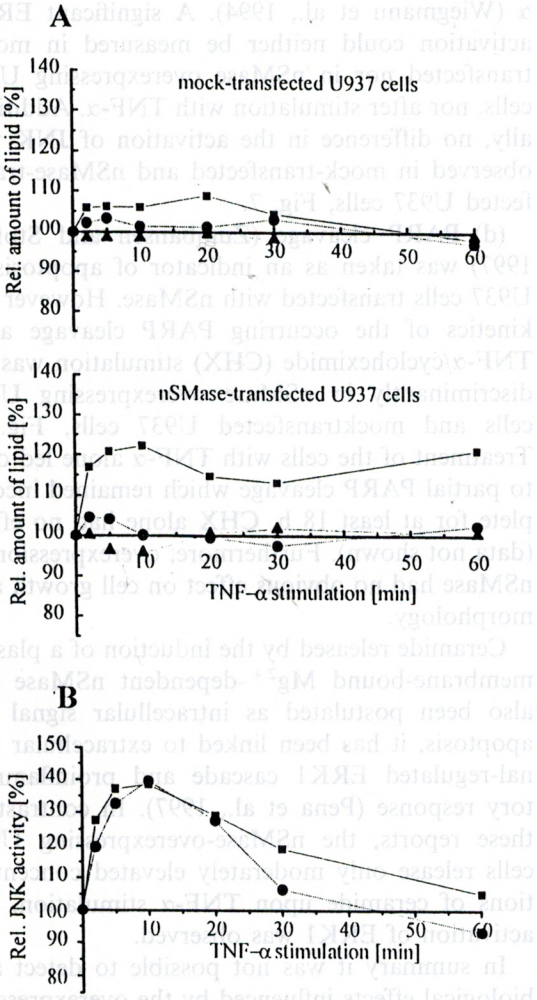

Fig. 7. Cellular response of neutral sphingomyelinase (nSMase)-overexpressing U937 cells challenged with tumor necrosis factor-α (TNF-α). (A) Kinetics of ceramide release after TNF-α stimulation of mock-transfected and nSMase-overexpressing U937 cells. Cells were stimulated with 100 ng/ml hTNF-α for the times indicated in the figure and lipids extracted as described (Otterbach and Stoffel, 1995). Ceramide (■), sphingomyelin (SPM) (●) and phosphatidylethanolamine (PE) (▲) were normalized to phosphatidylcholine. (B) Kinetics of JNK2 activation in mock-transfected (■) and nSMase-overexpressing U937 cells (●) after treatment with 100 ng/ml hTNF-α.

brain-specific activation process of nSMase or an additional nSMase in brain. Nerve growth factor receptor ($p75^{NTR}$) belongs to the TNFR family and regulates cell death of retinal neurons in early development (Schütze et al., 1992). Later in development the binding of its ligand NGF to $p75^{NTR}$ selectively activates NF-κB (Carter et al., 1996) and ERK1 and 2 (Volonte et al., 1993). NF-κB activity is constitutively present in nuclei of neurons and inducible in the cytoplasm and the synapse (O'Neill and Kaltschmidt, 1997). Deficiency of NGF leads to neuronal death. It has been reported that binding of NGF to $p75^{NTR}$ activates sphingomyelinase with the release of ceramide (Dobrowsky et al., 1995; Frade et al., 1996). Also ceramide released by exogenously added bacterial sphingomyelinase has been described to overcome NGF deprivation (Ito and Horigome, 1995). The high specific activity of nSMase in neuronal tissue might thus be essential for neuronal survival.

The characterization of the molecular properties of the newly discovered nSMase will facilitate studies to unravel the mechanism of the agonist stimulated activation on nSMase and induced degradation of SPM.

The regulated activation of nSMase might play an important role in maintaining the well known equilibrium between SPM and cholesterol in the plasma membrane and thus play a role in the

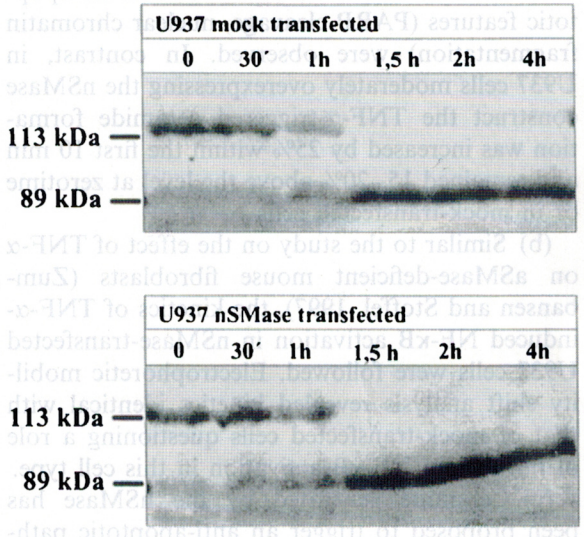

Fig. 8. Kinetics of PARP cleavage after treatment of transfected U937 cells with 200 ng/ml hTNF-α and 10 μg/ml cycloheximide (CHX).

regulation of plasma membrane fluidity which might be relevant for signal transduction. Treatment of CHO-7 cells with bacterial SMase led to the mobilization and intracellular accumulation of cholesterol followed by an inhibition of sterol regulatory element binding protein (SREBP) proteolysis and of transcription of sterol regulatory element (SRE)-containing genes (Scheek et al., 1997). The molecular characterization of this and on additional nSMase will also clarify its contribution to the generation of ceramide and its function as a lipid second messenger in signaling pathways including that of other sphingolipid metabolites. Like the asmase 'knock out' mouse a nsmase null allelic mouse model will provide insight into the complex regulation of the enzymatic activity and into other cellular functions of nSMase.

References

Adam, D., Wiegmann, K., Adam-Klages, S., Ruff, A., Krönke, M., 1996. J. Biol. Chem. 271, 14617–14622.

Adam-Klages, S., Adam, D., Wiegmann, K., Struve, S., Kolanus, W., Schneider-Mergener, J., Krönke, M., 1996. Cell 86, 937–947.

Barenholz, Y., Roitman, A., Gatt, S., 1966. J. Biol. Chem. 241, 3731–3737.

Bucher, P., Karplus, K., Moeri, N., HoLmann, K., 1996. Comput. Chem. 20, 3–23.

Carter, B.D., Kaltschmidt, C., Kaltschmidt, B., Offenhauser, N., Bohm-Matthaei, R., Baeuerle, P.A., Barde, Y.A., 1996. Science 272, 542–545.

Chatterjee, S., Ghosh, N., 1989. J. Biol. Chem. 264, 12554–12561.

Divecha, N., Irvine, R.F., 1995. Cell 80, 269–278.

Dobrowsky, R., Jenkins, G., Hannun, Y., 1995. J. Biol. Chem. 270, 22135–22142.

Dressler, K.A., Mathias, S., Kolesnick, R.N., 1992. Science 255, 1715–1718.

Frade, J., Rodriguez-Tebar, A., Barde, Y., 1996. Nature 383, 166–168.

Hannun, Y.A., Bell, R.M., 1989. Science 243, 500–507.

Hannun, Y.A., Obeid, L.M., 1995. Trends Biochem. Sci. 20, 73–77.

Ito, A., Horigome, K., 1995. J. Neurochem. 65, 463–466.

Jarvis, W.D., Kolesnick, R.N., Fornari, F.A., Taylor, R.S., Gerwitz, D.A., Grant, S., 1994. Proc. Natl. Acad. Sci. USA 91, 73–77.

Klenk, E., 1935. Z. Physiol. Chem. Hoppe-Seyler 235, 24–36.

Kolesnick, R., van Golde, D.W., 1994. Cell 77, 325–328.

Konnerth, A., Llano, I., Armstrong, C.M., 1990. Proc. Natl. Acad. Sci. USA 87, 2662–2665.

Kümmel, T.A., Schroeder, R., Stoffel, W., 1997. J. Neuropath. Exp. Neurol. 56, 171–179.

Machleidt, T., Wiegmann, K., Henkel, T., Schütze, S., Baeuerle, P., Krönke, M., 1994. J. Biol. Chem. 269, 13760–13765.

Maruyama, E.N., Aima, M., 1989. J. Neurochem. 52, 611–618.

Mathias, S., Dressler, K.A., Kolesnick, R.N., 1991. Proc. Natl. Acad. Sci. USA 88, 10009–10013.

Newrzella, D., Stoffel, W., 1992. Biol. Chem. Hoppe-Seyler 373, 1233–1238.

Niemann, A., 1914. Jahrbuch Kinderheilkd. 79, 1–10.

Obeid, L.M., Linardic, C., Karolak, L.A., Hannun, Y.A., 1993. Science 259, 1769–1771.

Olivera, T., Bukley, N.E., Spiegel, S., 1992. J. Biol. Chem. 267, 26121–26127.

O'Neill, L., Kaltschmidt, C., 1997. Trends Neurosci. 20, 252–258.

Otterbach, B., Stoffel, W., 1995. Cell 81, 1053–1061.

Pena, L.A., Fuks, Z., Kolesnick, R., 1997. Biochem. Pharmacol. 53, 615–621.

Pereira, L., Desnick, R.J., Adler, D.A., Disteche, C.M., Schuchman, E.H., 1991. Genomics 9, 229–234.

Pick, L., 1927. Med. Klin. 23, 1483–1488.

Quintern, L., Schuchman, E., Levran, O., Suchi, M., Ferlinz, K., Reinke, H., Sandhoff, K., Desnick, R., 1989. EMBO J. 8, 2469–2473.

Raines, M.A., Kolesnick, R.N., Golde, D.W., 1993. J. Biol. Chem. 268, 14572–14575.

Rao, B.G., Spence, M.W., 1976. J. Lipid Res. 17, 506–515.

Scheek, S., Brown, M.S., Goldstein, J.L., 1997. Proc. Natl. Acad. Sci. USA 94, 11179–11183.

Schuchman, E.H., Suchi, M., Takahashi, T., Sandhoff, K., Desnick, R.J., 1991. J. Biol. Chem. 266, 8531–8539.

Schütze, S., Potthoff, K., Machleidt, T., Berkovic, D., Wiegmann, K., Krönke, M., 1992. Cell 71, 765–776.

Spence, M.W., 1993. Adv. Lipid Res. 26, 3–23.

Tomiuk, S., Hofmann, K., Nix, M., Zumbansen, M., Stoffel, W., 1997. Proc. Natl. Acad. Sci. USA 95, 3638–3643.

Volonte, C., Loeb, D.M., Greene, L.A., 1993. J. Neurochem. 61, 664–672.

Watts, J.D., Gu, M., Polverino, A.J., Patterson, S.D., Aebersold, R., 1997. Proc. Natl. Acad. Sci. USA 94, 7292–7296.

Wiegmann, K., Schütze, S., Machleidt, T., Witte, D., Krönke, M., 1994. Cell 78, 1005–1015.

Zumbansen, M., Stoffel, W., 1997. J. Biol. Chem. 272, 10904–10909.